

RESEARCH PAPER



Adenovirus and Oxaliplatin cooperate as agnostic sensitizers for immunogenic cell death in colorectal carcinoma

J. Milburn Jessup^{a,b,*}, Mohamed Kabbout^{a,b,*}, Nikolay Korokhov^c, Alex Joun^{a,b}, Ann E. Tollefson^d, William S. M. Wold^d, and Abid R. Mattoo^{a,b}

^aInova Schar Cancer Institute, Falls Church, VA, USA; ^bSchool of Systems Biology, George Mason University, Fairfax, VA, USA; ^cBioReliance, Rockville, MD, USA; ^dDepartment of Molecular Microbiology and Immunology, Saint Louis University School of Medicine, St. Louis, MO, USA

ABSTRACT

Treatments with cytotoxic agents or viruses may cause Immunogenic Cell Death (ICD) that immunize tumor-bearing hosts but do not cause complete regression of tumor. We postulate that combining two ICD inducers may cause durable regression in immunocompetent mice. ICD was optimized *in vitro* by maximizing calreticulin externalization in human colorectal carcinoma (CRC) cells by exposure to mixtures of Oxaliplatin (OX) and human adenovirus (AdV). Six mm diameter CT26 or 4T1 carcinomas in flanks of BALB/c mice were injected once intratumorally (IT) with OX, AdV or their mixture. Tumor growth, Tumor-Infiltrating Lymphocytes (TIL), nodal cytotoxicity, and rejection of a viable cell challenge were measured. Tumors injected IT once with an optimum mixture of 80 μ M OX – AdV 25 Multiplicity of Infection (MOI) in PBS buffer were 17–29% the volume of control tumors. When buffer was changed from PBS to 5% dextrose in water (D5W), volumes of tumors injected IT with 80 μ M OX-AdV 25 MOI were 10% while IT OX or AdV alone were 32% and 40% the volume of IT buffer-treated tumors. OX-AdV IT increased CD3+ TIL by 4-fold, decreased CD8+ PD-1+ TIL from 79% to 19% and induced cytotoxicity to CT26 cells in draining node lymphocytes while lymphocytes from CT26-bearing untreated mice were not cytotoxic. OX-AdV IT in D5W caused complete regression in 40% of mice. Long-term survivors rejected a contralateral challenge of CT26. The buffer for Oxaliplatin is critical. The two ICD inducer mixture is promising as an agnostic sensitizer for carcinomas like colorectal carcinoma.

ARTICLE HISTORY

Received 17 July 2019
Revised 17 August 2019
Accepted 5 September 2019

KEYWORDS

Adenovirus; immunogenic cell death; complete response; rectal carcinoma; calreticulin; CT26; 4T1; Oxaliplatin

Introduction

Our laboratory has focused on using viruses to inhibit tumor growth because of their potential to deliver agents that may target functions that are not easily druggable with small molecules. Early efforts developed a non-replicating virus and then a replicating virus that targeted cancer stem cells through inhibition of a low expression pluripotency transcription factor.¹ Such vectors often induce transient or continuous inhibition of growth of established tumors in preclinical models but not complete regression. As a result, another approach must be used in preclinical models to cause complete responses that translate to useful clinical therapies.

Casares et al.² first reported that a cytotoxic agent may initiate a death program that primes adaptive immunity to tumor by demonstrating that Doxorubicin-induced a caspase-dependent cell death program *in vitro* in mouse CT26 rectal carcinoma cells that generated protective immunity to challenge with viable CT26 cells. CT26 is a chemically induced rectal adenocarcinoma that is immunogenic but will, by itself, always overcome endogenous immune responses to kill the host.³ Since classic apoptosis is non-immunogenic, this chemotherapeutic death was termed Immunogenic Cell Death (ICD) and later described as a programmed form of

necrosis.⁴ Tesniere et al.⁵ subsequently reported that Oxaliplatin induced a similar immune response and that externalization of Calreticulin was essential for ICD. Yamano et al.⁶ found that incubation with high Multiplicities of Infection (MOI) of human adenoviruses (AdV) also induced ICD in the CT26 prevention model. It seemed reasonable that if adenoviruses stimulate innate immunity in mice that are immunodeficient,^{7–9} then they might be combined with Oxaliplatin in immunocompetent mice to induce a stronger response than what develops with ICD monotherapy. As a consequence, we sought to determine whether Oxaliplatin, a known ICD inducer that is also part of standard of care for colorectal carcinoma in patients,^{10,11} and our AdV would produce a stronger therapeutic response in immunocompetent BALB/c mice to control cancer growth.

A major advantage of ICD is that it is an agnostic immunization because it does not require prior knowledge of neoantigens. The necroptosis activates pathways developed to defend against pathogens or other danger signals for the host. Activation of Pathogen Associated or Damage Associated Molecular Pattern pathways by AdVs, chemotherapy, radiation or other damaging agents causes endoplasmic reticulum (ER) stress that externalizes Calreticulin (CRT) with its cargo of neoantigens to the plasma membrane before cell death.^{12,13} ATP is released along with

CONTACT J. Milburn Jessup ✉ jessupjm69@yahoo.com 📍 8012 Coach Street, Potomac, MD 20854, USA

*These authors contributed equally

📄 Supplemental data for this article can be accessed on the [publisher's website](#).

© 2019 The Author(s). Published with license by Taylor & Francis Group, LLC.

This is an Open Access article distributed under the terms of the Creative Commons Attribution-NonCommercial-NoDerivatives License (<http://creativecommons.org/licenses/by-nc-nd/4.0/>), which permits non-commercial re-use, distribution, and reproduction in any medium, provided the original work is properly cited, and is not altered, transformed, or built upon in any way.

HMBG1 and other chaperones to attract infiltrating dendritic cells and assist with the presentation of the neoantigens through the CD91 pathway to dendritic cells. Dendritic cells then activate and stimulate cytotoxic T lymphocytes to migrate back to tumor deposits to kill malignant cells (see reviews by Kepp et al.^{4,14}). Tumorcidal innate immune effector cells are also activated during ICD.⁴ Results in preclinical models^{15–17} and the clinic^{18,19} strongly support the development of this innate and adaptive immune response during ICD but suggest that a checkpoint inhibitor is usually needed to develop complete regression. Also, one ICD inducer is not sufficient usually to achieve regression, but repeated treatments with either the ICD inducer or the checkpoint inhibitor must be employed to support immune responses sufficient to control tumor growth.²⁰

Our postulate is that complete regression in progressively growing tumors may be achieved by combining two ICD inducers in appropriate buffer to induce a stronger response than either one alone does. To that end, we have developed a human AdV that is immunogenic in both humans and mice. This AdV replicates in human colorectal carcinoma cells and infects but does not replicate in mouse cells at clinically useful MOI. Our approach is to optimize a mixture of AdV with Oxaliplatin for Calreticulin externalization *in vitro* on human CRC cell lines. Then, inject this mixture intratumorally (IT) into 6 mm diameter progressively growing mouse CT26 or 4T1 carcinomas in immunocompetent BALB/c mice. This approach initially caused anti-tumor immunity and reproducible cytostasis in growth. However, analysis of the interaction of Oxaliplatin with AdV demonstrated that the buffer initially used for Oxaliplatin⁵ decreased AdV infectivity so that a clinical buffer is needed to improve viral function. Use of the clinical buffer in a single IT mixture leads to complete remission in 40% of mice after a single IT treatment.

Materials and methods

Cells, chemicals, and cytotoxicity assay

Human colorectal carcinoma lines Clone A, CX-1 and LS174T were described in Zhang et al.¹ Mouse rectal adenocarcinoma CT26 cells and breast carcinoma 4T1 cells were obtained from American Type Culture Collection (Manassus, VA). Authentication was assessed by IDEXX BioAnalytics (Columbia, MO). Oxaliplatin was obtained from Selleck Chemicals (Houston, TX). Antibodies were obtained to mouse CD3 (Abcam), FITC CD8, APC-eFluor 780 PD-1, PerCP-eFluor 710 EOMES (ThermoFisher, Waltham, MA), Cy3-Calreticulin (BIOSS, Woburn, MA), Anti-RIP3 (phospho-S227) antibody (Abcam, Cambridge, MA), anti-Phospho-RIP-1 (Ser166) (D1L3S) and Anti-Phospho-MLKL (Cell Signal Technologies, Danvers, MA). Western blots were performed as described by Zhang et al.¹ Cytotoxicity of CT26 cells by nodal lymphocytes was measured by LIVE/DEAD™ Cell-Mediated Cytotoxicity Kit, for animal cells (ThermoFisher) according to the manufacturer's instructions. Inhibitory concentration 50% (IC50) used the WST-1 viability reagent from Sigma-Aldrich/Roche on monolayers of cells treated in 3 day cultures as described in text using the manufacturer's protocol. ATP and HMBG1 concentrations in spent medium were determined by assays from ThermoFisher and LSBio

(Seattle, WA), respectively, according to the manufacturer's instructions. Culture Medium was obtained from ThermoFisher.

RT-PCR, restriction endonuclease digestion and qRT-PCR

Was performed and analyzed per the method of Zhang et al.¹ with primers listed in Supplementary File Table 1 and obtained from Eurofins USA (Louisville, KY).

Virus construction and preparation

Lentivirus was created and propagated as described by Zhang et al.¹ The adenoviruses used the pAdEasy-1 with pShuttle and pUC19 plasmids (all from Addgene, Watertown, MA) respectively, to insert genes into the deleted E1 and E3 regions. The 1.2 kb NANOGP8 promoter controlling E1A and E1B expression and restricting virus replication to cells that express NANOGP8, E1A, and E1B genes were added into E1 region. A *Swa*I restriction enzyme site was created in the pAdEasy-1 plasmid to allow addition of genetic material to the E3 region. For Ad5/3-NP2 AdV the CMV promoter, copGFP, H1 promoter, NANOGP8 shRNA from the lentivirus were added in the E3 region with an Ad5/3 fiber. For the Ad5/3-NP2.ADP virus PVIII, 12.5K, X, Y, ADP, ADP polyA region were added in addition to the genes from Ad5/3-NP2. PVIII encodes a structural adenoviral protein and the E3 promoter that controls expression of the ADP protein.²¹ Drs. Tollefson and Wold graciously supplied both a pMT2 plasmid with Ad5 ADP inserted at the *Eco*RI site as well as Adenovirus ADP Rabbit antisera (Rabbit # 100578) generated against a peptide that represent amino acids 63–77 of the Ad2 ADP sequence that was used to confirm the presence of ADP protein in western blots at 1:400 dilution. The modified pUC19 and pShuttle were constructed by NEB (New England Biolabs, Ipswich, MA) Assembly according to manufacturers' instructions. The different inserts were introduced into pAdEasy by homologous recombination using BJ5183 *E. coli* bacteria according to He et al.²²

AdV were prepared by infecting 70% confluent 293T17 cells with viral lysate and harvesting cells and medium after 72–96 h. Cells and medium were subjected to three freeze-thaw cycles and lysate clarified by centrifugation at 2,000 g for 10 min at 4°C followed by ultracentrifugation at 20000 g for 2 h at 4°C with pellet passed through 0.22 μm PES filter and stored at –80°C in aliquots. MOI used infectious units determined by direct fluorescence TCID50 assay on human Clone A cell monolayers.²³

Animal experiments

Animal experiments with lentivirus and adenovirus in 90 six week old male NOD/SCID mice were performed under the protocol LEC-011 approved by the NCI Animal Care and Use Committee. Experiments with mouse CT26 cells and mouse 4T1 cells in 76 six week old BALB/c female mice were performed under protocol 1050837–1 approved by the George Mason University Institutional Animal Care and Use Committee. Mice were obtained from Charles River Laboratories. NOD/SCID mice in groups of 9–12 mice were

injected with 3×10^6 viable cells in the right flank subcutaneously and then injected with lentivirus or adenovirus when tumors were 5 mm in diameter. Tumors were measured three times a week and volumes calculated by $0.5 \times \text{Length} \times \text{Width}^2$ in mm. For experiments with mouse rectal carcinoma CT26 or mouse breast 4T1 carcinoma 5×10^5 viable cells were injected subcutaneously in groups of 5–7 mice in the right flank and tumor volumes measured as described for the NOD/SCID mice.

Tumor-infiltrating lymphocytes and cytotoxicity

Tumor and axillary lymph nodes were harvested aseptically from euthanized mice and one half, in PBS, was dissociated by passage through a sterile 40 gauge stainless steel mesh with a sterile spatula in PBS. Dissociated cells were then washed three times in PBS. TIL were analyzed by flow cytometry on a FACSCalibur cytometer (Becton Dickinson, Franklin Lakes, NJ) using protocols and dilutions recommended by Thermofisher using CD8, PD-1, and EOMES antibodies listed above. The data was collected with CellQuest (Becton Dickinson) and analyzed by Flowing Software (Turku Center for Biotechnology, Turku, Finland).

The other half of each tumor was fixed in 10% Neutral Buffered Formalin for 48 hr and then changed to 70% Ethanol. Fixed tumor was then embedded, sectioned and stained for CD3 + T cells with DAB counterstain by Histoserve, Inc. (Germantown, MD) using Thermofisher anti-mouse CD3 antibody. Sections were imaged and CD3+ cells enumerated in the digital images with NIH ImageJ version 2.0.0-rc-69/1.52i Build 26910ad53f as described in text. Results are presented as Mean \pm SEM/mm².

Calreticulin externalization and viral infectivity

1×10^5 human A or CX-1 cells were cultured in 12 well culture plates (Corning) for 5 days with Ad5/3-NP2 at an MOI of 25 and Oxaliplatin concentrations from 0 – 160 μ M as indicated in text. Cells were harvested and dissociated with Versene solution and then analyzed by flow cytometry for GFP positivity and Calreticulin externalization with Cy3-anti-calreticulin (BIOSS) at 1:50 for 60 min at 23°C and cells were washed three times before imaging in the FL2 channel on the FACSCalibur cytometer. In other experiments, Calreticulin and GFP positive cells were imaged by static cytometry with an inverted epi-fluorescence microscope (Amscope) and then enumerated with ImageJ as described above for TIL. Significance was determined by ANOVA analyzed in GraphPad Prism v7 with Holm-Sidak correction for multiple comparisons.

Statistical analysis

Significance was set at a two-tailed $P < .05$. The volume of tumors was calculated as described above. All analyses were conducted in Prism V.7 (GraphPad Software, Inc). Tumor volumes were Log₁₀ transformed and then individual tumor growth determined by linear regression. The method of Hather et al.²⁴ was then used to estimate Rate-Based

Treatment/Control (T/C) rates at a specified date. This approach uses all data from all mice and also enables Power calculations through 100 simulation bootstrapping as described by Hather et al.²⁴ Volumes are presented as Mean \pm SEM with comparisons of volumes by two-way ANOVA and Rate-Based T/C's at 21 days (CT26) or 19 days (4T1) by one-way ANOVA. All multiple comparisons are corrected by Holm-Sidak correction.

Results

The need for a replicating virus

Our group¹ originally developed a nonreplicating lentivirus as an anti-cancer stem cell virus. LV shNp8-1 contained an H1-driven shRNA that targets the pluripotency transcription factor NANOGP8 and inhibits spherogenicity and the side population in vitro and the growth of transduced human CRC cells in immune deficient NOD/SCID mice. NANOGP8 is a retrogene of the NANOG family of pluripotent transcription factors that is expressed in ~70% of CRC liver metastases as well as most human carcinomas, leukemias, and sarcomas.²⁵ IT injection of established CX-1 xenografts with LV shNp8-1 controlled tumor growth in NOD/SCID mice for more than 7 days but then the tumor outgrew the effect (Supplemental Figure 1, Panel A). The number of copies of the H1-shRNA gene was measured by PCR in CX-1 tumors at 3 days and at euthanasia. Four to 17 LV copies/6.6 pg tumor DNA were present 3 days after IT injection but decreased to 0.01 – 0.44 LV copies/6.6 pg DNA 12 days later at euthanasia. Although host mice may have deleted transduced tumor cells, CX-1 GFP negative cells that were not transduced grew out and overcome any transient growth inhibition. Thus, a replicating virus was necessary to get a more sustained inhibition of tumor growth in the xenograft model.

We then developed Ad5/3-NP8 with the AdEasy system that was E1, E3 region deleted²² but inserted wild type E1A-E1B genes in the E1 region, added a type 3 knob on the type 5 fiber, and placed the H1- shRNA and CMV- GFP reporter from the lentivirus in the E3 region (Supplemental Figure 2). A replicating control virus (Ad5/3-WT) was created that was similar to Ad5/3-NP8 but had a scrambled shRNA (Supplemental Figure 2). Simultaneously, we created Ad5/3-NP2 a conditionally replicating AdV in which a 1 Kb mini-promoter from the NANOGP8 retrogene was inserted upstream of the E1A gene with the same H1- shRNA and CMV- GFP reporter as in Ad5/3-NP8 in the E3 deleted region (Supplemental Figure 2). The viruses were tested for their ability to inhibit cancer stem cell function as defined by the work of Zhang et al.¹ in which stemness is measured by the ability of cells to form spheroids of more than 50 cells from single cells after 9 days of culture in suspension in serum-free medium. Both Ad5/3-NP8 and Ad5/3-NP2 are non-oncolytic but inhibit stem cell function in human Clone A cells (Figure 2D). When Ad5/3-NP2 or Ad5/3-WT were injected into CX-1 and LS174T xenografts, both continuously reduced tumor growth by 30% but did not cause regression (Supplemental Figure 1B, C). Since Ad5/3-WT was as active as Ad5/3-NP2 (Supplemental Figure 1B, C), inhibition of xenograft growth is likely due to host innate immunity to the AdV.^{7–9} If this is the case, then we postulated a need to 1)

make the AdV oncolytic and 2) use it as an immunogen in immune competent mice.

Preparation of an oncolytic Ad5/3-NP2.ADP AdV

The Ad5/3-NP2 virus was re-engineered to include the Adenovirus Death Protein (ADP) under the control of the E3 promoter as well as a redesigned mini-promoter that contained 1.2 Kb of the NANOGP8 promoter. This Ad5/3-NP2.ADP virus produces shRNA to NANOGP8 (Figure 1A) and inhibits total NANOG gene expression (Figure 1B). Both Ad5/3-NP2 and Ad5/3-NP2.ADP inhibit NANOG transcripts by 50–70% in Clone A and CX-1 cells at 5 days of culture (Figure 1C). The Ad5/3-NP2.ADP virus is more active in inhibiting spherogenicity than Ad5/3-NP2 since it essentially stops the formation of spheroids in CX-1 cells while the Ad5/3-NP2 virus only inhibits spherogenicity by ~50% and Ad5/3-NP8 with the E1A wild type promoter and the same shRNA to NANOGP8 inhibits spherogenicity by 90% (Figure 1D). Ad5/3-NP2.ADP is cytotoxic to human Clone A cells in the 3-day monolayer survival assay (Figure 1E). Since mouse cells neither support replication of human adenovirus nor express NANOGP8, both Ad5/3-NP2 and Ad5/3-NP2.ADP were used in subsequent in vivo experiments with mouse tumors as essentially interchangeable immunogenic agents.

Optimization of ICD in human CRC lines

Our approach to combining Oxaliplatin with our Ad5/3 viruses was to determine an optimal ratio for drug to virus that externalized Calreticulin. Calreticulin exposure on the plasma membrane is essential for ICD because Calreticulin chaperones nascent peptides along the lumen of the endoplasmic reticulum. During ER stress, the Calreticulin is externalized²⁶ and carries these peptides

as potential neoantigens that can be transferred to CD91 on dendritic cells for endocytosis and eventual presentation with Class I or II MHC molecules.²⁷ When Oxaliplatin and Ad5/3-NP2 were tested on human Clone A and human CX-1 cells in vitro for 5 days, the optimal ratio of Oxaliplatin and Ad5/3-NP2 for the percentage of cells expressing externalized Calreticulin was 80 μ M Oxaliplatin with 25 MOI of Ad5/3-NP2 (Figure 2A–E). Higher concentrations of Oxaliplatin inhibited AdV infectivity as indicated by a reduction in the percentage of cells infected as well as the intensity of GFP expression (Figure 2B–D). Interestingly, lower concentrations of Oxaliplatin combined with adenovirus induced gene expression of Type I and II interferons and TNF-alpha in human Clone A CRC (Figure 2F). However, it was important to have a slightly higher Oxaliplatin concentration to anticipate dilution within tumor tissue in vivo. Ad5/3-NP2.ADP is synergistic with Oxaliplatin for cell death because both 25 and 12.5 MOI of Ad5/3-NP2.ADP left shifted the IC₅₀ for Oxaliplatin from 9.8 μ M to 2.5 μ M or 0.3 μ M for 12.5 and 25 MOI Ad5/3-NP2.ADP, respectively (Figure 2E). Interestingly, high concentrations of Oxaliplatin cause Calreticulin externalization in Mouse CT26 cells (Supplemental Figure 3A) confirming Tesniere et al.⁵ while high MOI of AdV activates mixed lineage kinase domain like pseudokinase (MLKL) in mouse CT26 cells (Supplemental Figure 3B) that degrades plasma membranes during the final phases of necroptosis.²⁸ In addition, Oxaliplatin (Supplemental Figure 3C) and MOI of 12.5 and 25 of Ad5/3-NP2 increases expression of Type I and II interferons in mouse CT26 cells (Supplemental Figure 3D). At 3-days AdV releases ATP in vitro in both Clone A and CT26 cells (Supplemental Figure 4) and HMBG1 by ADV and the Oxaliplatin-AdV mixture (Supplemental Figure 5). As a result, Ad5/3-NP2.ADP is synergistic with Oxaliplatin in mouse CT26 cells even though Ad5/3-NP2.ADP is not directly cytotoxic to mouse CT26 cells at an MOI of 12.5 or 25 (Figure 2G). Thus, both Ad5/3 viruses enhance the

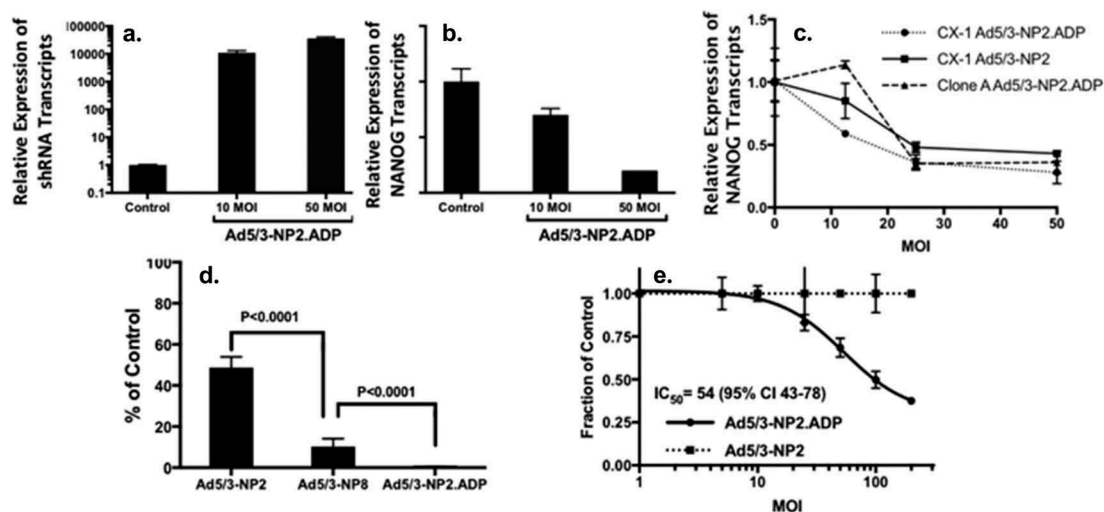


Figure 1. Ad5/3-NP2.ADP inhibits NANOG expression and cancer stem cell function. Panel A) Clone A cells infected with Ad5/3-NP2.ADP MOI 10 or 50 for 3 days in monolayer produce ds shRNA to NANOGP8 detected by qRT-PCR. Panel B) Clone A cells from Panel A also have lower total NANOG gene expression by qRT-PCR. Panel C) Clone A and CX-1 cells infected for 3 days with 10–50 MOI Ad5/3-NP2.ADP lower NANOG total gene expression more than Ad5/3-NP2 does in CX-1. Panel D) Ad5/3-NP2.ADP is more active in inhibiting spheroid formation in the Single Cell Spherogenic Assay in CX-1 cells than either Ad5/3-NP2 or Ad5/3-NP8 (similar to Ad5/3-NP2 except that it contains the wild type E1A). Panel E) IC₅₀ of Clone A cells in monolayer culture exposed to dilutions of the adenoviruses in a 3-day WST-1 assay. Means \pm SD are presented.

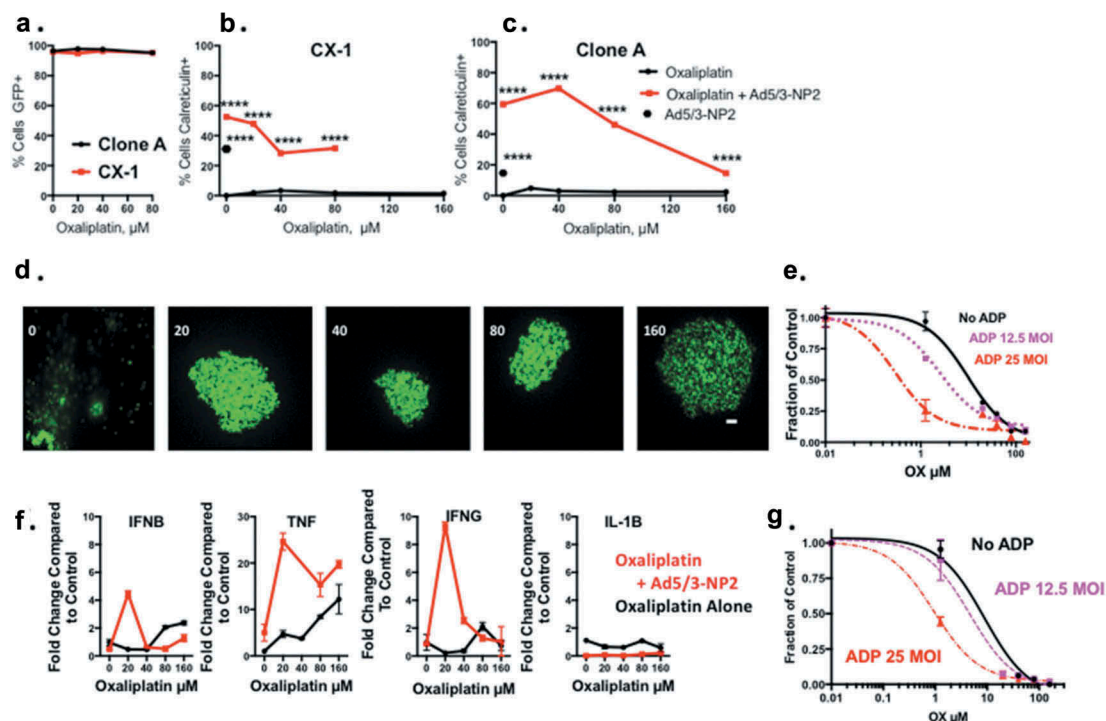


Figure 2. Synergy between oxaliplatin and adenovirus in human and mouse CRC for induction of ICD. 1×10^5 Clone A or CX-1 cells were cultured in 12 well culture plates for 5 days with Ad5/3-NP2 at an MOI 25 and OX from 0 – 160 μM as indicated in Panels A-C. Cells harvested and dissociated with Versene solution and then analyzed by flow cytometry for GFP positive cells (Panel A), for Calreticulin positive cells in CX-1 (Panel B) or Clone A (Panel C) by the combination of Oxaliplatin and virus. Red Line in Panels B and C is mixture of Oxaliplatin and virus; Black line is Oxaliplatin alone and () is 25 MOI virus alone. Mean \pm SD of % Calreticulin⁺ cells presented. Significance by two-way ANOVA analyzed in GraphPad Prism v7 with Holm-Sidak correction for multiple comparisons. **** $P < .0001$. Panel D) 500 CX-1 cells in 3-D culture for 7 days incubated with 25 MOI Ad5/3-NP2.ADP and the indicated concentrations of Oxaliplatin in μM . Panel E) 3-day WST-1 survival assay of Clone A cells incubated with Oxaliplatin or Oxaliplatin plus either 12.5 MOI or 25 MOI of Ad5/3-NP2.ADP with IC50's of 9.8 μM (95% CI 5.8 to 15.8 μM) for Clone A, 2.5 μM (95% CI 1.5 to 4.9 μM) Clone A with ADP 12.5 MOI and 1.0 μM (0.8 to 1.1 μM) Clone A with ADP 25 MOI. Panel F) Relative gene expression of IFNB, TNF-alpha, IFNG or IL-1B after 3-day exposure to Oxaliplatin alone or Oxaliplatin + Ad5/3-NP2 at 25 MOI in monolayer culture. Panel G) CT26 incubated with Oxaliplatin and the indicated MOI of Ad5/3-NP2.ADP in a 3-day WST-1 assay as in Panel E). IC50's for CT26 cells were 8.8 μM (95% CI 5.6 to 13.9), Oxaliplatin with 12.5 MOI virus is 4.7 μM (95% CI 3.0 to 7.4) and with 25 MOI virus is 0.95 μM 95% CI (0.9 to 1.1). Results are means \pm SD for Panels E and G and Means \pm SEM for Panel F.

ability of Oxaliplatin to induce ICD as measured by externalization of Calreticulin, induction of interferons and actual cell death not only in human CRC but also in mouse CT26 cells.

Initial effect of the Oxaliplatin-adenovirus mixture on CT26 and 4T1 carcinoma

Mouse rectal carcinoma CT26 and mouse breast carcinoma 4T1 tumors were established subcutaneously in the flanks of female BALB/c mice and injected IT when tumors were 6 mm diameter with a mixture of 80 μM Oxaliplatin mixed with 25 MOI of either Ad5/3-NP2 or Ad5/3-NP2.ADP. Six mm diameter tumors are oval to spherical and range in estimated total number of $1.5\text{--}6.1 \times 10^7$ CT26 cells with each CT26 cell an average of 15 μm in diameter. On average, we used 1×10^9 infectious units of AdV in a total volume of 100 μl injectate. This provides an estimated range of 16–65 MOI of AdV for the potential range of tumor volumes. Such an IT injection caused a marked decrease in growth that was initially cytostatic but did not cause regression (Figure 3A, B). However, when mice were euthanized 11 days after IT injection, there was a shift in CD8⁺ T cells from 79% PD-1⁺EOMES^{INT-High} in untreated CT26 tumor-bearing mice to 79% PD-1⁻EOMES^{Low} in IT Oxaliplatin-AdV injected tumors (Figure 3C, D). In addition, there was a four-fold increase in CD3⁺ Tumor-Infiltrating Lymphocytes (Figure 3E–G). Also, axillary node lymphocytes

from IT-treated CT26 tumor-bearing mice were cytotoxic to CT26 cells whereas lymphocytes from untreated CT26 tumor-bearing mice were significantly less cytotoxic to CT26 target cells than lymphocytes from normal littermate mice (Figure 3H). IT injection of the combination therapy cause a 77–79% reduction in volume of cancer in CT26-bearing mice and 83% in 4T1 bearing mice (Table 1). Thus, IT injection of a mixture of Oxaliplatin and AdV significantly reduced the growth of CT26 and 4T1 tumors in syngeneic mice, increased TIL and induced cytotoxicity in regional nodes but did not cause regression in any of the treated mice.

The importance of the buffer

Since Tesniere et al.⁵ used Phosphate-Buffered Saline for Oxaliplatin solutions, our first three experiments used the same buffer. However, since Oxaliplatin cross-links dsDNA and Adenovirus is a dsDNA virus, Oxaliplatin may inactivate AdV when mixed and incubated with AdV over time. The FDA requires that Oxaliplatin be administered in 5% dextrose in water (D5W) and not in chloride-containing solutions²⁹ because Chloride ion displaces the oxalate group in the presence of divalent cations and make Oxaliplatin more toxic.³⁰ We compared the effect of 80 μM Oxaliplatin in D5W or in the chloride-containing RPMI1640 on AdV infectivity in monolayers of Clone A cells. Both buffers had similar effects

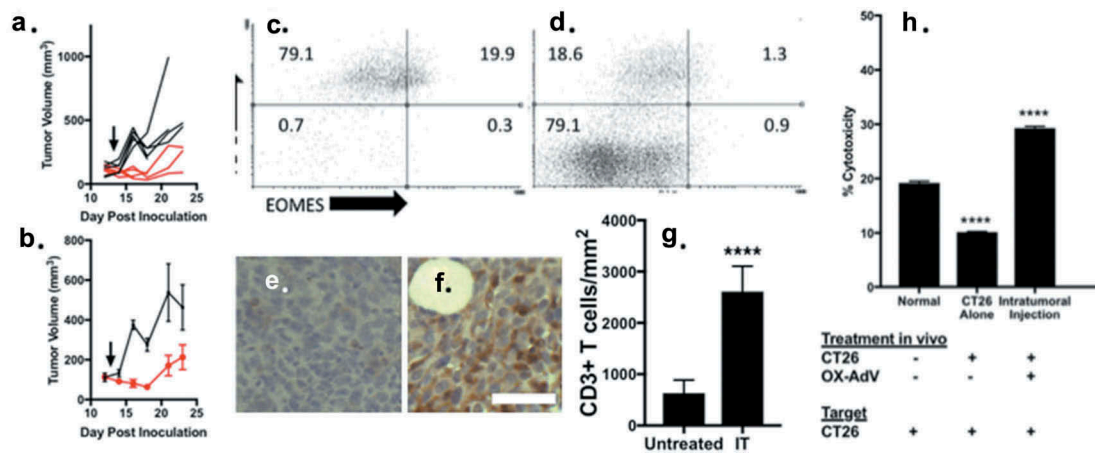


Figure 3. IT Ox-ADP increases T cell TIL and cytotoxicity to CT26. Mice in Experiment 1 from Table 1 were injected with $5E+5$ mouse CT26 cells and treated as described as in text. Panel A) tumors in individual mice are presented as a spider plot that demonstrates growth in each mouse. Black lines are controls and red lines are mice treated IT with Oxaliplatin and AdV. Panel B) mean volumes \pm SEM for mice in Panel A. Panels C and D) Mice were euthanized 11 days after IT treatment and tumors harvested, dissociated or formalin-fixed and flow cytometry was performed for CD8 + T cells, PD-1 and the intracellular Eomesodermin (EOMES) transcription factor as a marker of differentiation to exhaustion. Panel C) CD8 + T cells from Untreated CT26 were 79% PD-1⁺EOMES^{int-High}. Panel D) IT-treated tumors contained 79% CD8+ PD-1⁻EOMES^{Low} T cells that are either naïve or memory effector T cells. Panel E) the untreated CT26 stained for CD3 + T cells, Panel F) IT-treated CT26 tumor stained for CD3 + T cells. White bar = 50 μ m. DAB counterstaining for both C and D. Panel G) the mean \pm SEM of CD3 + T cells per mm² in six separate fields. Panel H) Lymphocytes from the draining axillary lymph nodes were suspended and incubated with CT26 cells at an effector:tumor cell ratio of 100:1. Normal lymphocytes were harvested from age-matched littermates that were not exposed to CT26 or virus. Cytotoxicity determined by Invitrogen Live-Dead Animal Cell Assay and *P* values determined by one-way ANOVA with Holm-Sidak multiple comparisons correction. **** *P* < .0001 compared to Untreated (Panel E) or Normal (Panel F) or Normal lymphocytes in (Panel H).

Table 1. Reproducible inhibition of CT26 rectal and 4T1 breast carcinoma in syngeneic BALB/c Mice.

| Experiment/Tumor | Treatment | Buffer | Rate-Based T/C ₂₁ | P | Power |
|------------------|---------------------|--------|------------------------------|----|-------|
| 1/CT26 | None | - | - | | |
| | OX 80 μ M + NP2 | PBS | 0.29 | ** | 0.96 |
| 2/CT26 | PBS | - | - | | |
| | OX 80 μ M + ADP | PBS | 0.23 | ** | 0.94 |
| Experiment/Tumor | Treatment | Buffer | Rate-Based T/C ₁₉ | P | Power |
| 3/4T1 | PBS | - | - | | |
| | OX 80 μ M + ADP | PBS | 0.17 | * | 0.97 |

Groups of 5–8 6 weeks old BALB/c female mice were injected with 5×10^5 viable CT26 (Experiments 1 and 2) or 4T1 (Experiment 3) cells in the right flank. When tumors were 6 mm in diameter, 0.10 ml of PBS containing 80 μ M Oxaliplatin (OX) with 25 MOI of Ad5/3-NP2 (NP2) (Experiment 1) or Ad5/3-NP2.ADP (ADP) in Experiments 2 and 3 was injected into the tumors. Tumors were measured three times a week and results are Mean \pm SEM. A spider plot of individual mice from Experiment 1 are presented in Figure 3A and B. Rate-based T/C at either 21 or 19 days is calculated by the method of Hather et al.²⁴ that uses all data from all mice with linear regression of log-transformed volumes. Significance is determined by one-way ANOVA with multiple comparison correction. Power provided by bootstrapping to model variance from heterogeneity of small samples. * *P* < 0.05, ** *P* < 0.01, *** *P* < 0.001, **** *P* < 0.0001. OX – Oxaliplatin, NP2 – Ad5/3-NP2, ADP – Ad5/3-NP2.ADP.

on cell cytotoxicity (Supplemental Figure 4A) but AdV infectivity was inhibited more in RPMI 1640 than in D5W (Supplemental Figure 4B, C). These results suggested that mixing Oxaliplatin and virus for less than 30 min in D5W before IT injection may improve the efficacy of the mixture. In the fourth experiment IT 80 μ M Oxaliplatin and 25 MOI Ad5/3-NP2.ADP in the 5% dextrose buffer reduced the growth of CT26 by 90% with 2 of 5 mice achieving clinical complete response by Day 24 (Figure 4A,C, Table 2). 80 μ M Oxaliplatin alone or Ad5/3-NP2.ADP reduced tumor growth by 68% and 60%, respectively (Figure 4A, Table 2). The median survivals of the virus alone, Oxaliplatin alone and Combination groups of 26, 33 and 34 days, respectively, were significantly longer than the 22-day median survival of controls (Figure 4B). The two complete responders in the combination Oxaliplatin-AdV group along with the two surviving mice in the AdV alone group along with age-matched

littermates were challenged in the contralateral flank 21 days after IT injection with 1×10^6 viable CT26 cells. All of the treated mice rejected the contralateral challenge whereas CT26 grew in all the normal age-matched control mice (Figure 4D). Thus, IT treatment induced tumor transplantation immunity, at least in the longer-term survivors. Interestingly, one of the complete responders in the combination Oxaliplatin-AdV treated group relapsed in the original tumor site when challenged with viable tumor and died later from disease (Figure 4B, C) while the other is a durable complete responder surviving more than 170 days from tumor implantation.

Discussion

Our data extend ICD as an agnostic immunization through two major findings. First, the combination of two ICD

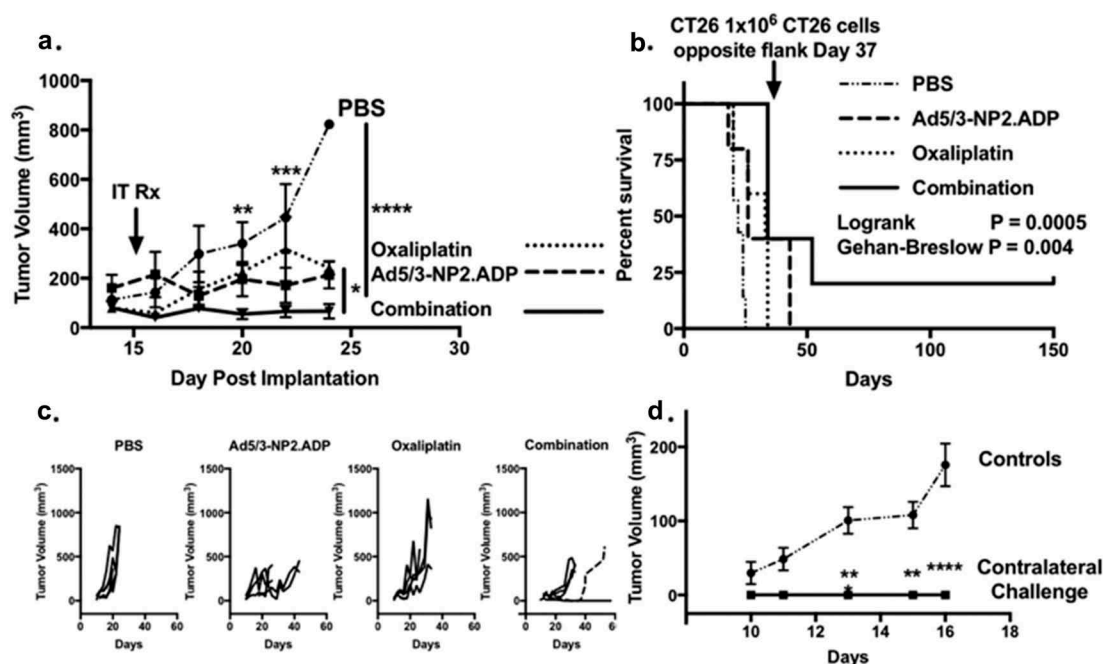


Figure 4. IT therapy with Oxaliplatin in D5W causes regression in CT26 carcinoma in BALB/c mice. Groups of 5–7 6 week old female mice were injected with 5×10^5 viable cells in the flank. When nodules were 6 mm diameter at day 16, Oxaliplatin (OX 80 μ M), Ad5/3-NP2.ADP (ADP) at 25 MOI or in combination was injected IT. Tumors were measured and analyzed as described in Table 1. Panel A) mean growth for each group analyzed up to Day 24. Panel B) Overall survival for each group with median survival and *P* values determined by Kaplan-Meier analysis. Panel C) Individual mouse plots of tumor volumes in each treatment group. Panel D) Rejection of 1×10^6 viable CT26 cells in the contralateral flank at day 37 by two complete responders in the OX+ADP group and two mice with small primaries in the ADP group. Controls are age-matched littermates. * *P* < .05, ** *P* < .01, *** *P* < .001, **** *P* < .0001.

Table 2. Buffer change increases effect of IT Oxaliplatin and Adenovirus.

| Experiment/ Tumor | Treatment | Buffer | Rate-Based | | |
|----------------------|---------------------|--------|-------------------|------|-------|
| | | | T/C ₂₁ | P | Power |
| 4/CT26 | PBS | PBS | - | - | |
| | ADP | D5W | 0.40 | **** | 0.94 |
| | OX 80 μ M | D5W | 0.32 | **** | 0.93 |
| | OX 80 μ M + ADP | D5W | 0.10 | **** | 0.80 |

Groups of 5–7 female BALB/c mice were injected with 5×10^5 viable mouse CT26 cells in the right flank. Mice were treated IT as described in Table 1 and Figure 4. Tumor volumes were analyzed as described in Table 1.

inducers is better than either one alone. In this report, we combine a chemotherapy agent with a biologic and demonstrate that in vivo the combination is significantly better than IT treatment with either Oxaliplatin or the virus alone. This combination is similar to the interaction of chemotherapy with ionizing radiation in patients treated with advanced cancer. Radiation therapy induces abscopal effects where lesions outside the radiation field regress.^{18,19} Without another systemic treatment, such regressions are considered to be due to the induction of anti-tumor immune responses. However, the abscopal effects of combining radiation therapy with systemic chemotherapy may be due to the systemic therapy rather than to an immune response that is hard to measure in vivo. The regression of uninjected cutaneous melanoma metastases in patients treated with intralesional injection of Talimogene Laherparepvec (T-VEC)³¹ combined with systemic ipilimumab, the anti-CTLA4 checkpoint inhibitor, clearly demonstrates that local immunization can be enhanced to cause distant responses throughout the host. However, to the best of our knowledge, our work is the first example of combining two ICD inducing agents into one single

intralesional therapy that enhances TIL, changes the majority of infiltrating CD8 + T cells from PD-1⁺ to PD-1⁻, and induces nodal cytotoxicity and transplantation resistance.

An interesting aspect of the therapy is that relatively low concentrations of 0.1–40 μ M Oxaliplatin with fixed doses of virus induced the highest externalization of Calreticulin (Figure 2B,C) as well as the highest gene expression of *IFNB*, *IFNG* and *TNF* genes (Figure 2F). However, we chose to use the Oxaliplatin concentration of 80 μ M for the intra-tumoral injection because 1) mouse CT26 cells and mouse 4T1 cells do not support replication of the adenovirus at MOI of 25 and 2) dilution of the injectate within a solid mass of tumor lead to lower concentrations of drug that still will be active. Nonetheless, it is clear that the combination of Oxaliplatin and AdV is synergistic for cell death in both human Clone A (Figure 2E) and mouse CT26 (Figure 2G) *in vitro* because there is a significant left shift in the IC₅₀ curves with the addition of the AdV.

Our data suggest that replicating virus in immune incompetent NOD/SCID mice is able to continuously inhibit the growth of human CRC xenografts where the nonreplicating lentivirus with the same payload could only temporarily retard the growth of CX-1 xenografts. While not directly tested, since the control adenovirus had the same effect as the experimental virus, it is likely that the host innate immune response to adenovirus slowed the growth of the xenograft. Type 5 adenovirus induces innate immune responses through MyD88/TLR⁹ or cGAS/STING⁸ that would account for the reduction in growth in NOD/SCID mice. Nishime et al.⁹ also demonstrated that NOD/SCID mice can activate NK cells to inhibit xenograft growth. Thus, innate immunity may be

important for viral effects on xenografts in immune incompetent mice but may not be able to cause rejection of established tumor.

Our treatment was initially developed against human CRC lines *in vitro* because our intended clinical use is in second-line treatment of advanced CRC. Sixty percent of CRC have few TIL or exclude T cells from entering the cancer and are considered cold and poorly responsive to checkpoint inhibitor therapy.^{32,33} If this ICD-based regimen induces strong immune/inflammatory responses in CRC that may be boosted further by checkpoint inhibitor therapy, then this therapy may be important for such other cold human malignancies as non-HER2+/TNBC breast, prostate, serous ovarian, thyroid carcinomas or Glioblastoma Multiforme.³³

Systemic chemotherapy, especially with anthracyclines or oxaliplatin, administered in multidrug regimens as standard of care may induce ICD and, as being tested now in clinical trials, lead to responses to checkpoint inhibitor therapy in cancers that generally do not respond to immunotherapy. However, the amount of Oxaliplatin in tumor or even normal tissue is likely too low to induce strong ICD. Systemic administration of the standard dose of Oxaliplatin 130 mg/m² over 2 h leads to a peak plasma concentration of ~10 µg/ml that is 25 µM.³⁴ Since the *t*_{1/2} was 30 min, the concentration of Oxaliplatin in tumor will be lower than 20 µM especially since 40% of the Oxaliplatin in plasma is quickly bound to plasma proteins.³⁵ Intratumoral injection of 80 µM Oxaliplatin puts at least twice the amount of the highest plasma concentration into tumor. Thus, intratumoral injection may be better than systemic for agnostic sensitization.

Our approach using intratumoral injection of a mixture of two agents is not as appealing as systemic treatment. However, IT injection by interventional radiologic techniques is safe.³⁶ Our intended use is for patients with advanced CRC in second-line therapy with liver or lung metastases. Hemorrhage is the major complication but occurs in less than 2% of over 20,000 procedures.³⁶ Procedure cost is \$5,000–10,000 while the cost of the checkpoint inhibitors is 5–10 times that.³⁷ The **advantage of IT injection** is that a high local concentration may be delivered safely without systemic toxicity, consistent with the concentrations needed to induce ICD. Although Oxaliplatin is water-soluble and might enter the systemic circulation, a 1 ml injection of 80 µM Oxaliplatin into a 2 cm liver metastasis will deliver 31.8 µg of oxaliplatin into the tumor which is less than the 60 µg of Oxaliplatin absorbed by a 2 cm metastasis with 1 cm liver margin during isolated liver perfusion.³⁸ Thus, IT injection is safe, unlikely to leak into the circulation but will provide a high concentration to induce ICD.

The limitations of this study that will be addressed in the near future include defining the effector cells in their contributions and most importantly whether the agnostic immunization presented here also induces responses to the Th1³⁹ and cytotoxic peptides⁴⁰ that have been previously identified in the CT26 model. Another limitation that needs to be addressed is whether the transplantation resistance has memory and is specific to CT26. Further work is also necessary to determine whether tumor in other locations in the host will limit the activity of adaptive immunity. Since two of the

survivors that rejected the contralateral challenge had residual cancer in their virus injected tumors, it is quite likely that the induced adaptive immunity may be strong enough to reject distant tumor. However, in summary, this work indicates that ICD is an immunization method that is agnostic to prior knowledge of neoantigens and that two ICD inducers are better than one.

Acknowledgments

The authors are grateful for the support and encouragement by Dr. Donald L. Trump, the former Chief Executive Officer of the Inova Schar Cancer Institute.



Disclosure of potential conflicts of interest

No potential conflicts of interest were disclosed.

Funding

Study supported by the Center for Cancer Research of the NCI for Project ZIA BC 011199 and by the Department of Defense Grant Number W81XWH-11-1-0327 as well as by philanthropic funds from the Inova Schar Cancer Institute. All subsequent immunology and the ADP virus work was supported by private philanthropic funds supplied by the Inova Schar Cancer Institute when it was led by Dr. Donald L. Trump. If need be, please use this paragraph under whatever title you want for the financial support that extends over the past 7 years.

ORCID

J. Milburn Jessup  <http://orcid.org/0000-0002-6884-1872>
Alex Joun  <http://orcid.org/0000-0002-4019-911X>

References

- Zhang J, Espinoza LA, Kinders RJ, Lawrence SM, Pfister TD, Zhou M, Veenstra TD, Thorgeirsson SS, Jessup JM. NANOG modulates stemness in human colorectal cancer. *Oncogene*. 2013;32:4397–405.
- Casares N, Pequignot MO, Tesniere A, Ghiringhelli F, Roux S, Chaput N, Schmitt E, Hamai A, Hervas-Stubbs S, Obeid M, et al. Caspase-dependent immunogenicity of doxorubicin-induced tumor cell death. *J Exp Med*. 2005;202:1691–701.
- Lechner MG, Saman S, Karimi SS, Barry-Holson K, Murphy KA, Church CH, Ohlfest JR, Hu P, Epstein AL. Immunogenicity of murine solid tumor models as a defining feature of *in vivo* behavior and response to immunotherapy. *J Immunother*. 2013;36:477–89.
- Kepp O, Senovilla L, Vitale I, Vacchelli E, Adjemian S, Agostinis P, Apetoh L, Aranda F, Barnaba V, Bloy N, et al. Consensus guidelines for the detection of immunogenic cell death. *Oncoimmunology*. 2014;3:e955691.
- Tesniere A, Schlemmer F, Boige V, Kepp O, Martins I, Ghiringhelli F, Aymeric L, Michaud M, Apetoh L, Barault L, et al. Immunogenic death of colon cancer cells treated with oxaliplatin. *Oncogene*. 2010;29:482–91.
- Yamano T, Kubo S, Fukumoto M, Yano A, Mawatari-Furukawa Y, Okamura H, Tomita N. Whole cell vaccination using immunogenic cell death by an oncolytic adenovirus is effective against a colorectal cancer model. *Mol Ther Oncolytics*. 2016;3:16031.
- Yamaguchi T, Kawabata K, Koizumi N, Sakurai F, Nakashima K, Sakurai H, Sasaki T, Okada N, Yamanishi K, Mizuguchi H. Role of MyD88 and TLR9 in the innate immune response elicited by serotype 5 adenoviral vectors. *Hum Gene Ther*. 2007;18:753–62.

8. Anghelina D, Lam E, Falck-Pedersen E. Diminished innate antiviral response to adenovirus vectors in cGAS/STING-deficient mice minimally impacts adaptive immunity. *J Virol.* 2016;90:5915–27.
9. Nishime C, Kawai K, Yamamoto T, Katano I, Monnai M, Goda N, Mizushima T, Suemizu H, Nakamura M, Murata M, et al. Innate response to human cancer cells with or without IL-2 receptor common γ -chain function in NOD background mice lacking adaptive immunity. *J Immunol.* 2015;195:1883–90.
10. Iveson TJ, Kerr RS, Saunders MP, Cassidy J, Hollander NH, Taberero J, Haydon A, Glimelius B, Harkin A, Allan K, et al. 3 versus 6 months of adjuvant oxaliplatin-fluoropyrimidine combination therapy for colorectal cancer (SCOT): an international, randomised, phase 3, non-inferiority trial. *Lancet Oncol.* 2018;19:562–78. doi:10.1016/S1470-2045(18)30144-X.
11. Goldberg RM, Gill S. Recent phase III trials of fluorouracil, irinotecan, and oxaliplatin as chemotherapy for metastatic colorectal cancer. *Cancer Chemother Pharmacol.* 2004;54:S57–64.
12. Panaretakis T, Kepp O, Brockmeier U, Tesniere A, Bjorklund AC, Chapman DC, Durchschlag M, Joza N, Pierron G, van Endert P, et al. Mechanisms of pre-apoptotic calreticulin exposure in immunogenic cell death. *Embo J.* 2009;28:578e590.
13. Panaretakis T, Joza N, Modjtahedi N, Tesniere A, Vitale I, Durchschlag M, Fimia GM, Kepp O, Piacentini M, Froehlich KU, et al. The co- translocation of ERp57 and calreticulin determines the immunogenicity of cell death. *Cell Death Differ.* 2008;15:1499e1509. doi:10.1038/cdd.2008.67.
14. Kepp O, Galluzzi L, Martins I, Schlemmer F, Adjemian S, Michaud M, Sukkurwala AQ, Menger L, Zitvogel L, Kroemer G. Molecular determinants of immunogenic cell death elicited by anticancer chemotherapy. *Cancer Metastasis Rev.* 2011;30:61–69.
15. Kosinsky Y, Dovedi SJ, Peskov K, Voronova V, Chu L, Tomkinson H, Al-Huniti N, Stanski DR, Helmlinger G. Radiation and PD-(L)1 treatment combinations: immune response and dose optimization via a predictive systems model. *J Immunother Cancer.* 2018;6:17.
16. Rios-Doria J, Durham N, Wetzel L, Rothstein R, Chesebrough J, Holowecyj N, Zhao W, Leow CC, Hollingsworth R. Doxil synergizes with cancer immunotherapies to enhance antitumor responses in syngeneic mouse models. *Neoplasia.* 2015;17:661–70.
17. Pflirschke C, Engblom C, Rickelt S, Cortez-Retamozo V, Garris C, Pucci F, Yamazaki T, Poirier-Colame V, Newton A, Redouane Y, et al. Immunogenic chemotherapy sensitizes tumors to checkpoint blockade therapy. *Immunity.* 2016;44:343–54.
18. Buchwald ZS, Wynne J, Nasti TH, Zhu S, Mourad WF, Yan W, Gupta S, Khleif SN, Khan MK. Radiation, immune checkpoint blockade and the abscopal effect: a critical review on timing, dose and fractionation. *Front Oncol.* 2018;8:612.
19. Siva S, MacManus MP, Martin RF, Martin OA. Abscopal effects of radiation therapy: a clinical review for the radiobiologist. *Cancer Lett.* 2015;356:82–90.
20. Ariyan CE, Brady MS, Siegelbaum RH, Hu J, Bello DM, Rand J, Fisher C, Lefkowitz RA, Panageas KS, Pulitzer M, et al. Robust antitumor responses result from local chemotherapy and CTLA-4 blockade. *Cancer Immunol Res.* 2018;6:189–200.
21. Tollefson AE, Scaria A, Saha SK, Wold WS. The 11,600-MW protein encoded by region E3 of adenovirus is expressed early but is greatly amplified at late stages of infection. *J Virol.* 1992;66:3633–42.
22. He TC, Zhou S, Da Costa LT, Yu J, Kinzler KW, Vogelstein B. A simplified system for generating recombinant adenoviruses. *Proc Natl Acad Sci USA.* 1998;95:2509–14.
23. Shiau AL, Liu PS, Wu CL. Novel strategy for generation and titration of recombinant adeno-associated virus vectors. *J Virol.* 2005;79:193–201.
24. Hather G, Liu R, Bandi S, Mettetal J, Manfredi M, Shyu WC, Donelan J, Chakravarty A. Growth rate analysis and efficient experimental design for tumor xenograft studies. *Cancer Inform.* 2014;13:65–72.
25. Fairbanks DJ, Fairbanks AD, Ogden TH, Parker GJ, Maughan PJ. NANOGP8: evolution of a human-specific retro-oncogene. *G3 (Bethesda).* 2012;2:1447–57.
26. Obeid M, Tesniere A, Ghiringhelli F, Fimia GM, Apetoh L, Perfettini JL, Castedo M, Mignot G, Panaretakis T, Casares N, et al. Calreticulin exposure dictates the immunogenicity of cancer cell death. *Nature Med.* 2007;13:54–61.
27. Salimu J, Spary LK, Al-Taei S, Clayton A, Mason MD, Staffurth J, Tabi Z. Cross-Presentation of the oncofetal tumor antigen 5T4 from irradiated prostate cancer cells—A key role for heat-shock protein 70 and receptor CD91. *Cancer Immunol Res.* 2015;3:678–88.
28. Tanzer MC, Matti I, Hildebrand JM, Young SN, Wardak A, Tripaydonis A, Petrie EJ, Mildenhall AL, Vaux DL, Vince JE, et al. Evolutionary divergence of the necroptosis effector MLKL. *Cell Death Differ.* 2016;23:1185–97.
29. Downloaded 11/15/2018 from FDA.gov: eloxatin-L-OHP FDA prescribing information 021759s012lbl.pdf – version 1.6 of the prescribing information for Eloxatin (Oxaliplatin).
30. Han CH, Khwaounjoo P, Hill AG, Miskelly GM, McKeage MJ. Predicting effects on oxaliplatin clearance: in vitro, kinetic and clinical studies of calcium- and magnesium-mediated oxaliplatin degradation. *Sci Rep.* 2017;7:4073.
31. Chesney J, Puzanov I, Collichio F, Singh P, Milhem MM, Glaspy J, Hamid O, Ross M, Friedlander P, Garbe C, et al. Randomized, open-label phase II study evaluating the efficacy and safety of Talimogene Laherparepvec in combination with ipilimumab versus ipilimumab alone in patients with advanced, unresectable melanoma. *J Clin Oncol.* 2018;36:1658–67.
32. Hegde PS, Karanikas V, Evers S. The where, the when, and the how of immune monitoring for cancer immunotherapies in the era of checkpoint inhibition. *Clin Cancer Res.* 2016;22:1865–74.
33. Cristescu R, Mogg R, Ayers M, Albright A, Murphy E, Yearley J, Sher X, Liu XQ, Lu H, Nebozhyn M, et al. Pan-tumor genomic biomarkers for PD-1 checkpoint blockade-based immunotherapy. *Science.* 2018;362(6411):pii: eaar3593.
34. Pieck AC, Drescher A, Wiesmann KG, Messerschmidt J, Weber G, Strumberg D, Hilger RA, Scheulen ME, Jaehde U. Oxaliplatin-DNA adduct formation in white blood cells of cancer patients. *Br J Cancer.* 2008;98:1959–65.
35. Brauckmann C, Wehe CA, Kieshauer M, Lanvers-Kaminsky C, Sprelling M, Karst U. The interaction of platinum-based drugs with native biologically relevant proteins. *Anal Bioanal Chem.* 2013;405:1855–64.
36. Cui Z, Wright JD, Accordino MK, Buono D, Neugut AI, Hu JC, Hershman DL. Safety, utilization, and cost of image-guided percutaneous liver biopsy among cancer patients. *Cancer Invest.* 2016;34:189–96.
37. Cost of a Biopsy - Consumer Information – costHelper. [accessed 2019 Apr 2]. <https://health.costhelper.com/biopsy.html>.
38. Zeh HJ 3rd, Brown CK, Holtzman MP, Egorin MJ, Holleran JL, Potter DM, Bartlett DL. A phase I study of hyperthermic isolated hepatic perfusion with oxaliplatin in the treatment of unresectable liver metastases from colorectal cancer. *Ann Surg Oncol.* 2009;16:385–94.
39. Casares N, Lasarte JJ, de Cerio AL, Sarobe P, Ruiz M, Melero I, Prieto J, Borrás-Cuesta F. Immunization with a tumor-associated CTL epitope plus a tumor-related or unrelated Th1 helper peptide elicits protective CTL immunity. *Eur J Immunol.* 2001;31:1780–89.
40. Huang AY, Gulden PH, Woods AS, Thomas MC, Tong CD, Wang W, Engelhard VH, Pasternack G, Cotter R, Hunt D, et al. The immunodominant major histocompatibility complex class I-restricted antigen of a murine colon tumor derives from an endogenous retroviral gene product. *Proc Natl Acad Sci USA.* 1996;93:9730–35.